Ontogeny and Multipotency of Neural Crest-Derived Stem Cells in Mouse Bone Marrow, Dorsal Root Ganglia, and Whisker Pad

Narihito Nagoshi,[1,2] Shinsuke Shibata,[1] Yoshiaki Kubota,[3] Masaya Nakamura,[2] Yasuo Nagai,[1] Etsuko Satoh,[1] Satoru Morikawa,[1,4] Yohei Okada,[1,6] Yo Mabuchi,[1] Hiroyuki Katoh,[2] Seiji Okada,[1,7] Keiichi Fukuda,[5] Toshio Suda,[3] Yumi Matsuzaki,[1] Yoshiaki Toyama,[2] and Hideyuki Okano[1,*]

[1]Department of Physiology
[2]Department of Orthopedic Surgery
[3]Department of Cell Differentiation
[4]Department of Dentistry and Oral Surgery
[5]Department of Regenerative Medicine and Advanced Cardiac Therapeutics
Keio University School of Medicine, 35 Shinanomachi, Shinjuku-ku, Tokyo 160-8582, Japan
[6]Department of Neurology, Nagoya University Graduate School of Medicine, 65 Tsurumai-cho, Showa-ku, Nagoya 466-8550, Japan
[7]SSP Stem Cell Unit, Graduate School of Medical Science, Kyushu University, 3-1-1 Maidashi, Higashi-ku, Fukuoka 812-8582, Japan
*Correspondence: hidokano@sc.itc.keio.ac.jp
DOI 10.1016/j.stem.2008.03.005

SUMMARY

Although recent reports have described multipotent, self-renewing, neural crest-derived stem cells (NCSCs), the NCSCs in various adult rodent tissues have not been well characterized or compared. Here we identified NCSCs in the bone marrow (BM), dorsal root ganglia, and whisker pad and prospectively isolated them from adult transgenic mice encoding neural crest-specific P0-Cre/Floxed-EGFP and Wnt1-Cre/Floxed-EGFP. Cultured EGFP-positive cells formed neurosphere-like structures that expressed NCSC genes and could differentiate into neurons, glial cells, and myofibroblasts, but the frequency of the cell types was tissue source dependent. Interestingly, we observed NCSCs in the aorta-gonad-mesonephros region, circulating blood, and liver at the embryonic stage, suggesting that NCSCs migrate through the bloodstream to the BM and providing an explanation for how neural cells are generated from the BM. The identification of NCSCs in accessible adult tissue provides a new potential source for autologous cell therapy after nerve injury or disease.

INTRODUCTION

The neural crest is a transient embryonic tissue that originates at the neural folds during vertebrate development. Neural crest cells delaminate from the dorsal neural tube and migrate to various locations, where they differentiate into a vast range of cells, including neurons and glial cells of the autonomic and enteric nervous systems, smooth muscle cells of the heart and great vessels, and bone and cartilage cells of the face (Le Douarin and Kalcheim, 1999).

From the embryonic period through adulthood, neural crest cells are generated by neural crest-derived stem cells (NCSCs), which

are self-renewing and multipotent, with the potential to differentiate into neurons, glial cells, and myofibroblasts (Morrison et al., 1999; Shah et al., 1996). NCSCs have been isolated from the embryonic sciatic nerve (Morrison et al., 1999) and boundary cap (BC) (Hjerling-Leffler et al., 2005) and the gut (Kruger et al., 2002), skin (Fernandes et al., 2004; Sieber-Blum et al., 2004; Wong et al., 2006), heart (Tomita et al., 2005), and cornea (Yoshida et al., 2006) of adult rodents. These reports demonstrate the presence of NCSCs in these tissues and suggest their existence in other adult tissues.

Several types of stem cells have been identified in adult tissues. For example, several groups have described multipotent stem cells in the bone marrow (BM), but the developmental origin and differentiation potential of these cells are unknown (D'Ippolito et al., 2004; Jiang et al., 2002; Ross et al., 2006). These stem cells are reported to generate neural cells and smooth muscle cells, which are known to originate from neural crest cells. Such observations led us to investigate whether some newly identified stem cells might be NCSCs. We examined this hypothesis by investigating various tissues of double-transgenic mice encoding Protein-0 (P0) and Wnt1 promoter-Cre/Floxed-EGFP, in which neural crest-derived cells express EGFP (Danielian et al., 1998; Kawamoto et al., 2000; Yamauchi et al., 1999).

Here, we prospectively isolated and compared neural crest-derived stem and progenitor cells from the BM of the lower extremities, dorsal root ganglia (DRG), and whisker pad (WP) of adult P0 and Wnt1 promoter-Cre/Floxed-EGFP mice. This is the first report identifying NCSCs in the BM of adult rodents. The existence of NCSCs was confirmed in all three tissues, and distinct differences among the NCSCs were revealed by comparing their proliferation capacity, differentiation potential, and gene expression profiles.

RESULTS

Distribution of EGFP-Positive Neural Crest-Lineage Cells in Embryonic and Adult P0 and Wnt1-Cre/Floxed-EGFP Mice

To examine the distribution of neural crest-derived cells in various tissues, we performed histological analyses of
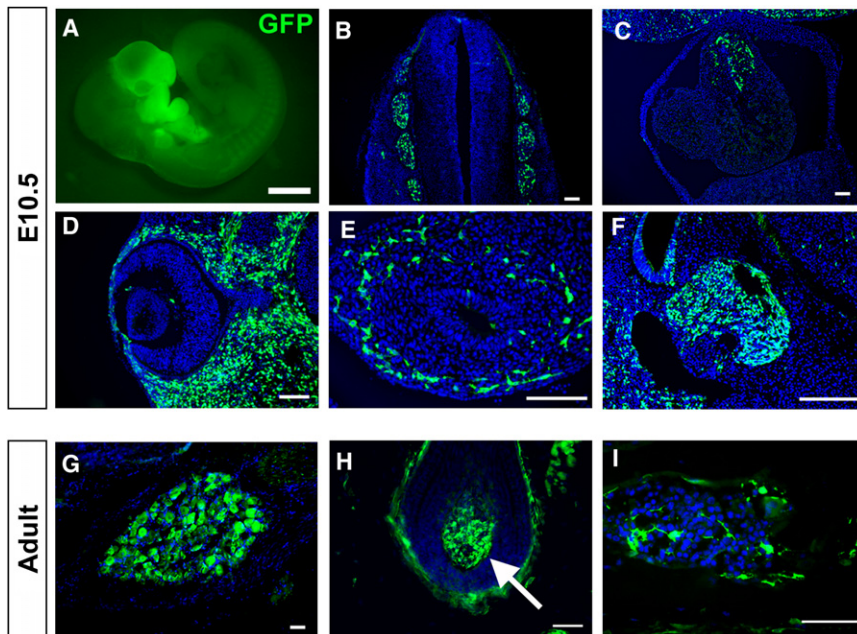
Figure 1. Expression Pattern of EGFP in P0-Cre/Floxed-EGFP Mice at E10.5 and the Adult Stage

(A) Whole-body observation of direct EGFP fluorescence in E10.5 mice.

(B–F) Anti-GFP immunostaining of E10.5 mice revealed EGFP^{+} cells in the DRG (B), outflow tract of the heart (C), optic mesenchyme (D), gut (E), and trigeminal ganglion (F).

(G–I) In 8-week-old adult mice, EGFP^{+} cells were detected in the DRG (G), dermal papilla in the whisker follicle (arrow in [H]), and BM of the tibia (I). Scale bars, 1 mm in (A) and 50 μm in (B)–(I).

P0-Cre/Floxed-EGFP mouse embryos and adults. P0 was originally identified as a Schwann cell-specific myelin protein (Lemke et al., 1988), but it is also expressed by migrating neural crest cells during the early embryonic period in chicks (Bhattacharyya et al., 1991). In this transgenic mouse, the transient activation of the P0 promoter induces Cre-mediated recombination, indelibly tagging neural crest-derived cells with EGFP expression (Kawamoto et al., 2000; Yamauchi et al., 1999). At E10.5, EGFP was observed in the pharyngeal arches, periocular region, and front nasal region, which contain neural crest-derived cells (Figure 1A) (Yamauchi et al., 1999). Anti-GFP immunostaining of E10.5 embryos revealed EGFP-positive (EGFP^{+}) cells in the DRG, outflow tract of the aorta, optic mesenchyme, gut, and trigeminal ganglia (Figures 1B–1F). In adult mice, EGFP^{+} cells were observed in the DRG, dermal papilla of whisker follicles, and BM of the tibia (Figures 1G–1I). As a negative control, we examined anti-GFP staining in single transgenic P0-Cre mice without the Floxed-EGFP reporter and detected no EGFP^{+} cells (data not shown), confirming the validity of the anti-GFP staining. Immunohistochemistry was also performed on various tissues from adult Wnt1-Cre/Floxed-EGFP mice, confirming the presence of EGFP^{+} cells in the DRG, dermal papilla, and BM (see Figure S1 available online). These observations suggest that EGFP[+] neural crest-derived cells migrate to and survive in various adult tissues.

Since neural crest-derived cells have not been previously reported in the BM, we analyzed the distribution of EGFP^{+} cells in the BM of P0-Cre/Floxed-EGFP mice by immunohistochemistry. It is unlikely that EGFP expression was induced by the ectopic expression of P0, since we did not detect P0 protein in the BM (Figure S2). In the BM of P0-Cre/Floxed-EGFP mice, EGFP^{+} cells were detected along blood vessels, especially the vasculature located near the inner surface of the bone cortex (Figures 2A–2C). In whole-mount specimens, these EGFP^{+} cells were positive for both PECAM-1 and SMA, markers for endothelial cells and smooth muscle cells (Figures 2E–2L), and quantitative analysis revealed that 3.85% and 6.23% of the EGFP^{+} cells

in the BM were positive for PECAM-1 and SMA, respectively. The contribution of EGFP^{+} cells to the vascular endothelial structure was also confirmed by flow-cytometric analysis (Figure 2D) and whole-mount immunohistochemistry with other vascular markers (Figures 2M–2X). Although a portion of vascular smooth muscle cells are known to be derived from the neural crest, neural crest-derived cells have not been reported in the vascular endothelium in previous studies (Etchevers et al., 2001; Joseph et al., 2004). To corroborate our observations, we examined the BM in adult Wnt1-Cre/Floxed-EGFP mice. Although a similar number of EGFP^{+} cells was observed, the EGFP^{+} cells did not express endothelial cell or smooth muscle cell markers (Figures S1C and S1D). Thus, our detailed analyses using two lines of transgenic mice demonstrated the presence of neural crest-derived cells in the BM, but their contribution to blood vessel formation remains unclear.

NCSCs Migrate from the Trunk Dorsal Neural Tube to the Aorta-Gonad-Mesonephros Region and Circulate in the Blood during Embryonic Development

To elucidate the migration route of EGFP^{+} cells from the trunk dorsal neural tube to the BM, we focused on the aorta-gonad-mesonephros (AGM) region in P0 and Wnt1-Cre/Floxed-EGFP mice. During development, the first adult-type hematopoietic stem cells (HSCs) are generated at E10.5 in the AGM region and migrate via the blood stream to the BM in the late embryonic period (Medvinsky and Dzierzak, 1996; Muller et al., 1994). Mesenchymal stem cells (MSCs) are also generated in the AGM region at E11.0, migrate in the blood stream, and are found in the neonatal BM (Mendes et al., 2005). We therefore hypothesized that neural crest-derived cells take a similar route to the BM, migrating from the dorsal neural tube to the AGM region, from which they then travel through the blood stream to the BM. Anti-GFP immunostaining revealed EGFP^{+} cells migrating from the trunk dorsal neural tube to the AGM region in E11.0 P0-Cre/Floxed-EGFP mice (Figure 3A). These EGFP^{+} cells were 100% positive for p75 and 50.6% positive for Sox10, both known as NCSC markers (Paratore et al., 2001; Stemple and Anderson, 1992) (Figures 3B and 3C), suggesting that a portion of the EGFP^{+} cells in the AGM region were NCSCs. At E12.5, most of the EGFP^{+} cells were positive for tyrosine hydroxylase
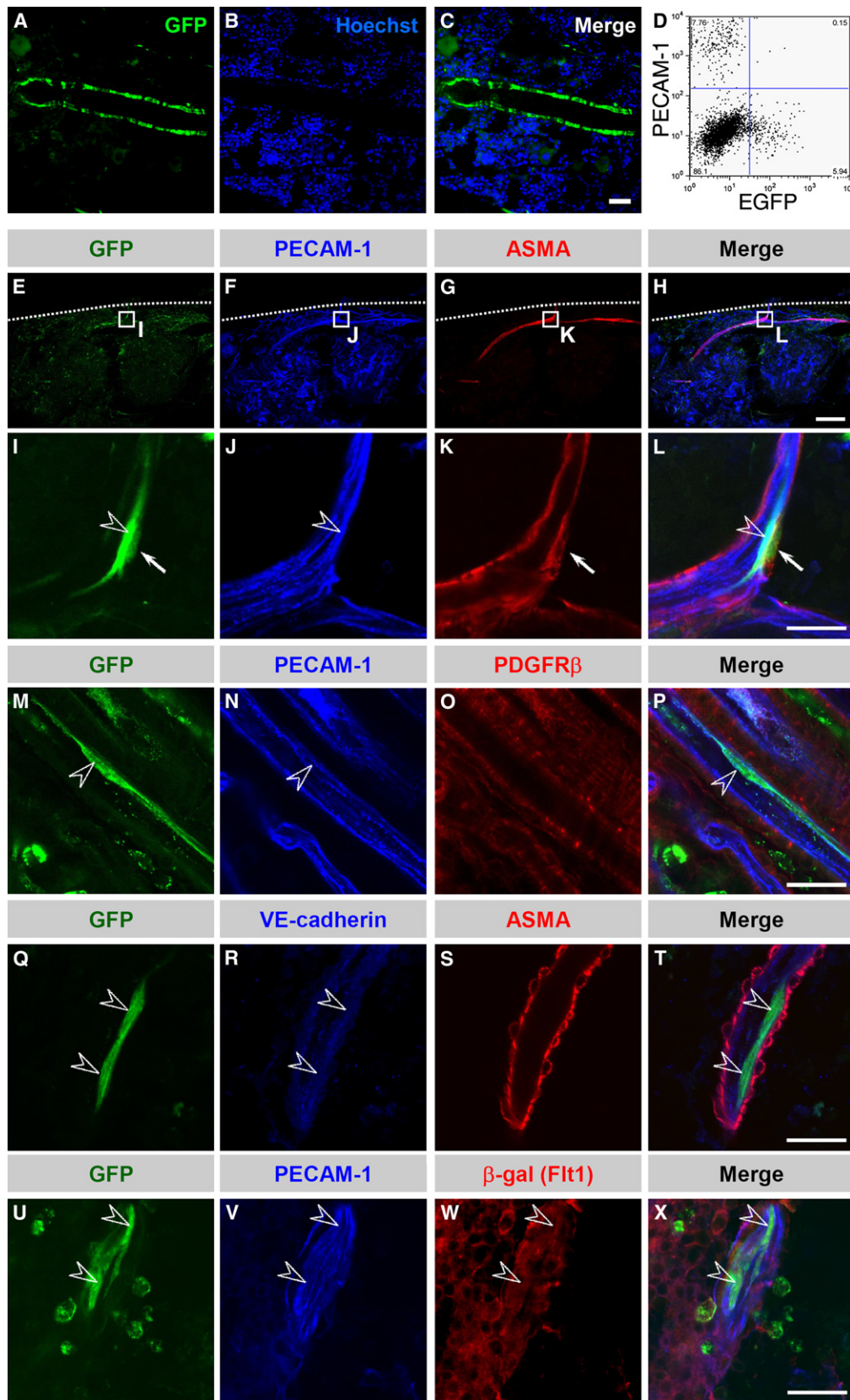
(TH), a marker of catecholaminergic neurons that make up the para-aortic plexus (Figure 3D), raising the possibility that EGFP⁺ Sox10⁻ cells at E11.0 were neuroblasts that differentiated into TH⁺ neurons at E12.5. However, the small number of TH⁻ EGFP⁺ cells that invaded the aorta were positive for p75 and Sox10 (Figures 3E–3H), suggesting that the cells entering the blood vessel were NCSCs. None of the EGFP⁺ cells at the periphery of aorta were positive for GFAP (Figure 3I), ruling out the possibility that the EGFP⁺ cells are newly arrived Schwann cells that are migrating along the vasculature. EGFP⁺ p75⁺ cells were also observed in peripheral blood at E12.5 by immunohistochemistry (Figures 3J and 3K), and flow-cytometric analysis of the blood taken from E13.5 to E15.5 mice detected EGFP⁺ cells (Figure 3L). In E14.5 mice, immunohistochemistry revealed EGFP⁺ Sox10⁺ cells in the fetal liver (Figures 3M and 3N). After E18.5, no EGFP⁺ cells were detected in the circulating blood (Figure 3L). Similar results were observed in the AGM region, peripheral blood, and fetal liver in Wnt1-Cre/Floxed-EGFP mice (Figure S3). These observations suggest that NCSCs migrate in the blood to the BM via the AGM region, specifically during E12.5–E15.5, similar to HSCs.

Sphere-Forming Capability of Neural Crest-Derived Cells from Adult Mice

To compare neural crest-derived cells from the DRG, WP, and BM, cells from these tissues were collected from postnatal 2-, 4-, 8-, and 13-week-old P0-Cre/Floxed-EGFP mice, and their EGFP expression was analyzed by flow cytometry. The frequency of EGFP⁺ cells from each source was highest at 2 weeks of age and decreased over time (Figures 4A and 4B). The same result was observed in Wnt1-Cre/Floxed-EGFP mice (Figure S4A). Interestingly, the number of EGFP⁺ cells collected from the BM increased when the bones were treated with collagenase. Since collagenase releases BM cells that adhere tightly to the bone (Funk et al., 1994), this suggests that the neural crest-derived cells observed histologically were tightly associated with the BM surface.

The formation of neurosphere-like spheres from neural crest-derived tissue has been reported (Fernandes et al., 2004; Tomita et al., 2005; Yoshida et al., 2006) using culture procedures similar to neurosphere-culture protocols for cells of the central nervous system (CNS) (Reynolds and Weiss, 1992). To confirm the capability of neural crest-derived cells to proliferate and form spheres, EGFP⁺ and EGFP⁻ cells from the DRG, WP, and BM of 8-week-old P0-Cre/Floxed-EGFP mice were collected by flow cytometry and cultured at a density of 5×10^3 cells/ml (Hulspas et al., 1997) in serum-free sphere-forming

medium containing human epidermal growth factor (EGF), human fibroblast growth factor 2 (FGF2), and B27. The EGFP⁺ cells proliferated to form spheres that were morphologically similar to CNS neurospheres after 14 days (Figure 4C). When cultured at the same density, the highest number of spheres was formed from cells derived from the DRG and the lowest from the BM (Figure 4D). Cultured EGFP⁻ cells derived from the DRG and BM did not form spheres, but those from the WP did, albeit at a much lower frequency than the EGFP⁺ cells (Figure 4D). Sphere-forming capacity and tissue-specific sphere-forming efficacy in cells from adult Wnt1-Cre/Floxed-EGFP mice were similar to those from P0-Cre/Floxed-EGFP mice (Figures S4B and S4C). These results indicate that neural crest-derived cells capable of proliferating into spheres exist in the adult DRG and BM in addition to the WP, which has been previously reported.

Spheres Derived from Each Adult Tissue Contain Multipotent NCSCs

Previous reports have characterized NCSCs by their ability to self-renew and their capacity for multilineage differentiation (multipotency) into neurons, glial cells, and myofibroblasts (Morrison et al., 1999; Shah et al., 1996). To evaluate the differentiation potential of EGFP⁺ spheres generated from sorted EGFP⁺ cells, we cultured EGFP⁺ spheres from the three tissue sources of adult P0-Cre/Floxed-EGFP mice for 10 days in 10% serum-containing differentiation medium. The differentiated cells were identified by triple immunostaining: neurons by β-III tubulin, glial cells by glial fibrillary acidic protein (GFAP), and myofibroblasts by SMA. EGFP⁺ spheres from all three sources demonstrated trilineage differentiation potential (Figure 5A), but the differentiation preference differed depending on the tissue source (Table 1). Most of the DRG-derived spheres showed trilineage differentiation potential (NGM, 74.6%), but the frequency was significantly lower in the WP- and BM-derived spheres (NGM, 7.3% and 3.3%, respectively). The WP-derived spheres displayed a bilineage differentiation tendency into neurons and myofibroblasts (NM, 91.6%), while most BM-derived spheres differentiated into myofibroblasts (M, 64.6%), suggesting that EGFP⁺ cells derived from the WP and BM are mostly lineage-restricted progenitors, with only a small percentage possessing multilineage differentiation potential. In addition, when EGFP⁺ DRG-derived spheres were cultured in differentiation medium containing 5-bromo-2′-deoxyuridine (BrdU) (Figure 5B), all three resulting cell types (N, M, and G) were positive for BrdU. Therefore, these three cell types from DRG-derived spheres probably originated from mitotic precursor cells within the

Figure 2. EGFP⁺ Cells Contribute to Vascular Endothelial and Smooth Muscle Cells in the BM of P0-Cre/Floxed-EGFP Mice

(A–C) EGFP⁺ cells were detected along vasculature in the tibia.

(D) Representative EGFP- and PECAM-1-gated flow-cytometric analysis chart. To prevent the contamination of macrophages, CD45⁺ cells were removed before analysis.

(E–L) Triple immunohistochemistry for GFP, PECAM-1, and SMA in whole-mount specimens. Note the abundant EGFP⁺ cells around the inner surface of the bone cortex (outer surface indicated by dotted lines). (I–L) High-magnification views of the boxed areas in (E)–(H), respectively. Note the EGFP⁺ endothelial cells (arrowheads) and smooth muscle cells (arrows).

(M–P) Triple immunohistochemistry for GFP, PECAM-1, and PDGFRβ, a marker for pericytes and smooth muscle cells. The arrowhead indicates EGFP⁺ PECAM-1⁺ endothelial cells.

(Q–T) EGFP⁺ cells were also positive for VE-cadherin, a marker for endothelial cells (arrowheads).

(U–X) In triple-transgenic mice encoding P0-Cre/Floxed-EGFP/Flt1^{lacZ}, EGFP⁺ cells were positive for PECAM-1 and β-gal (arrowheads). Flt1 is expressed in endothelial and hematopoietic cells. Scale bars, 50 μm in (A)–(C), 200 μm in (E)–(H), and 20 μm in (I)–(X).

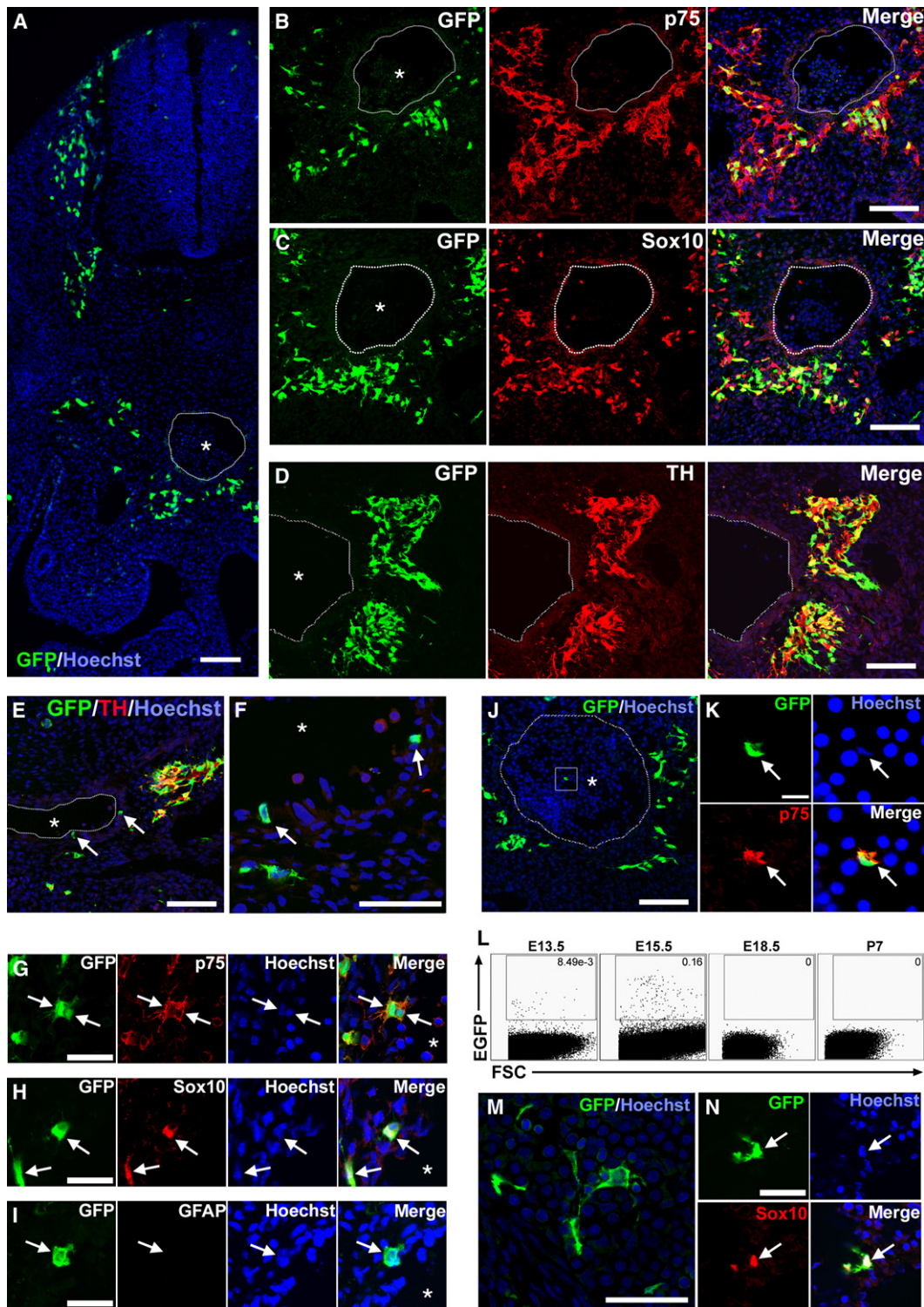**Figure 3. Histological Analyses of the AGM Region and Flow-Cytometric Analyses of Peripheral Blood in P0-Cre/Floxed-EGFP Mice**

(A) At E11.0, EGFP+ cells detected by anti-GFP antibodies were seen migrating from the dorsal neural tube into the AGM region. The region enclosed in a dashed line with an asterisk indicates the aorta.

(B and C) Double immunohistochemistry of the AGM region revealed that EGFP+ cells were positive for p75 (B) and partially colocalized with Sox10 (C), indicating that EGFP+ cells in the embryonic AGM region expressed NCSC markers.

(D–F) At E12.5, most EGFP+ cells had differentiated into TH-positive catecholaminergic neurons (D), but some EGFP+ TH− cells invaded the aorta (arrows in [E] and [F]).
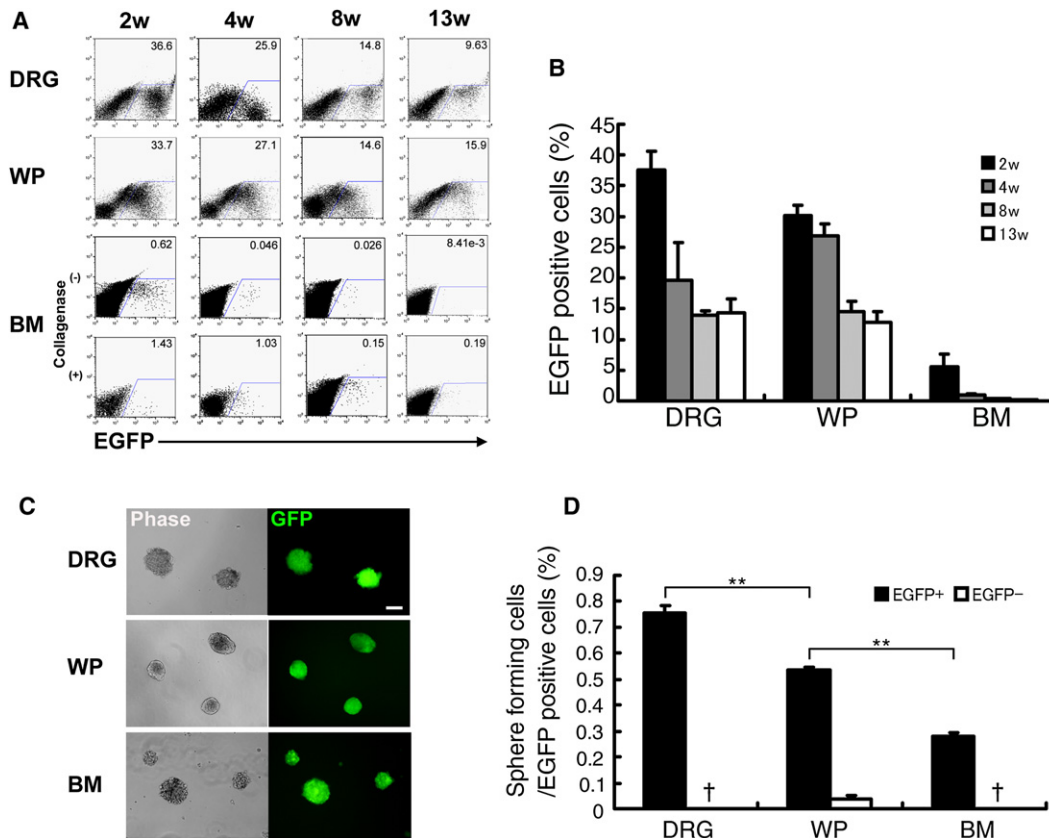
Figure 4. Isolation and Sphere-Forming Capacity of Neural Crest-Lineage Cells Derived from the DRG, WP, and BM in Adult P0-Cre/Floxed-EGFP Mice

(A) Representative EGFP-gated flow-cytometric analysis charts of cells from the DRG, WP, and BM of postnatal 2-, 4-, 8-, and 13-week-old mice. In the BM, the number of collected EGFP$^+$ cells increased with collagenase treatment.

(B) The number of collected EGFP$^+$ cells from all three sources decreased with age (mean ± SEM, n = 3 per group).

(C) Phase-contrast and direct EGFP-fluorescent images showing spheres formed from EGFP$^+$ cells after 14 days in culture. Scale bar, 50 μm.

(D) The percentage of sphere-forming cells found in each tissue source was assessed by culturing EGFP$^+$ and EGFP$^-$ cells from each source at a cell density of 5×10^3 cells/ml and counting the number of spheres formed (mean ± SEM; n = 3 per group; **p < 0.01; †, no sphere observed). The highest percentage of sphere-forming cells was observed in the DRG, and the WP was the only source with EGFP$^-$ cells capable of forming spheres.

spheres and did not represent contamination of postmitotic cells from the original tissue.

Recent reports have questioned the validity of "clonal density" cultures (Jessberger et al., 2007; Singec et al., 2006), demonstrating that CNS neurospheres are motile structures that can fuse even at cellular concentrations previously regarded as "clonal" (Hulspas et al., 1997). To assess the possible effects of sphere fusion in our culture protocol, we examined the differentiation of spheres cultured in medium containing 0.8% methylcellulose (Figures S5A–S5C). This method, which we previously reported (Yoshida et al., 2006), effectively prevents sphere fusion, resulting in spheres that are more than 90% clonal. Differentiation studies of these clonal spheres yielded results similar to those shown in Table 1 (Figure S5D), indicating

that the influence of sphere fusion was quite limited. Results from adult Wnt1-Cre/Floxed-EGFP mice corroborated data from adult P0-Cre/Floxed-EGFP mice, revealing the formation of clonal spheres from the DRG, WP, and BM that possessed a similar differentiation preference (Figures S4B–S4E).

To assess the self-renewal capacity of the EGFP$^+$ spheres, secondary sphere-forming assays were conducted. EGFP$^+$ spheres derived from each tissue source of P0-Cre/Floxed-EGFP mice were independently placed into one well of a 96-well plate, dissociated into single cells, and cultured in sphere-forming medium. The frequency of secondary sphere formation was highest in cells derived from the DRG (Figure 5C), confirming that, of these three sources, the DRG contains the highest frequency of NCSCs.

(G–I) At E12.5, most EGFP$^+$ cells at the periphery of the aorta were positive for p75 and Sox10 but negative for GFAP.

(J and K) EGFP$^+$ p75$^+$ cells were observed in the peripheral blood of E12.5 mice (boxed area in [J] magnified in [K]).

(L) EGFP-gated flow-cytometric analysis charts of embryonic and postnatal blood cells. EGFP$^+$ cells were detected from E13.5 and E15.5, but not at E18.5 or after birth. Transverse axis indicates forward scatter (FSC).

(M and N) At E14.5, EGFP$^+$ cells were observed in the liver. Some were positive for Sox10, indicating that NCSCs exist in the liver. Scale bars, 100 μm in (A)–(F), (J), and (M); 50 μm in (G)–(I), and (N); and 20 μm in (K).
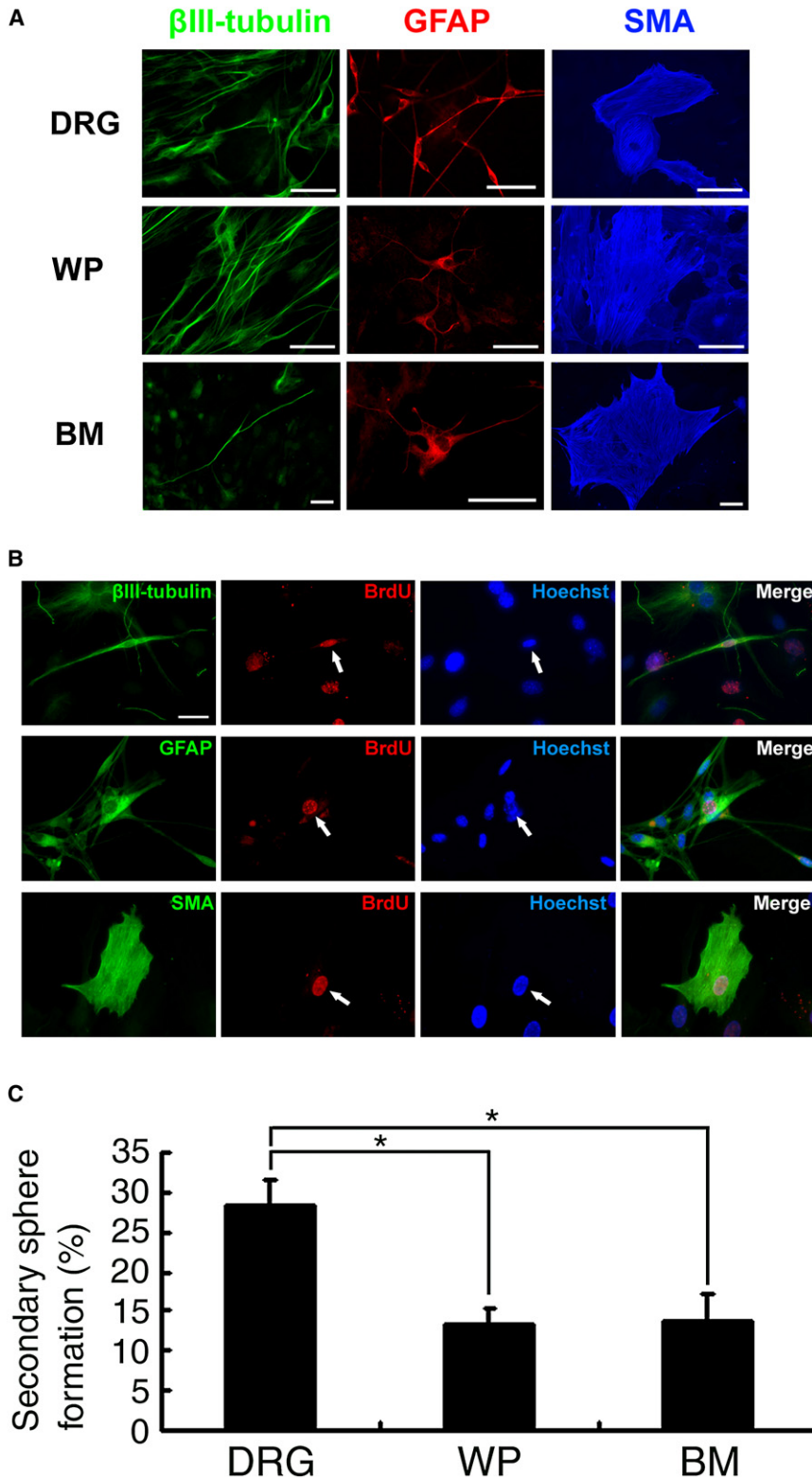
Figure 5. Differentiation and Secondary Sphere-Forming Capacity of EGFP⁺ Spheres Derived from the DRG, WP, and BM in Adult P0-Cre/Floxed-EGFP Mice

(A) EGFP⁺ spheres formed from each tissue source differentiated into neurons, glial cells, and myofibroblasts. Scale bars, 50 μm.

(B) DRG-derived spheres were cultured in medium containing BrdU. Cells double positive for BrdU and each cell-type-specific marker were observed. Scale bar, 25 μm.

(C) When these spheres were dissociated, the DRG-derived cells formed the greatest number of secondary spheres, indicating their high capacity for self-renewal (mean ± SEM; n = 3 per group; *p < 0.05).

EGFP mice were analyzed by semiquantitative RT-PCR for various markers, especially neural crest-associated genes (Figure 6A). The following were prepared from each adult tissue source: noncultured EGFP⁻ and EGFP⁺ cells, cultured spheres, and cells differentiated from spheres. The noncultured cells showed varying tissue-source-dependent gene expression patterns. EGFP⁺ cells from the DRG strongly expressed the known NCSC markers *Sox10* and *p75*. Although their expression of the neural crest markers *Snail*, *Slug*, *Twist*, *Sox9*, and *Pax3* was lower or undetectable compared to EGFP⁻ cells, most of these markers were expressed after culture. The expression of neural crest-associated genes was quite similar in EGFP⁺ and EGFP⁻ cells from the WP, whereas in the BM, their expression was significantly higher in EGFP⁺ cells compared to EGFP⁻ cells.

For the EGFP⁺ spheres, although the expression frequencies of neural crest-associated genes differed, the spheres from all three tissues generally expressed most of the neural crest-associated genes. By comparison, CNS neurospheres derived from the E14.5 striatum did not express the neural crest-associated genes *Snail*, *Slug*, *Twist*, *p75*, or *Pax3*. They expressed *sox9* and *sox10* as expected, since these genes are also deeply involved in development of the CNS (Stolt et al., 2003, 2004). *Nkx6.1* is a well-known marker expressed in the ventral half of the neural tube during early development (Jensen et al., 1996). EGFP⁺ cells and spheres did not express *Nkx6.1*, in contrast to its strong expression in embryonic stem cell-derived neurospheres ventralized by the sonic hedgehog protein (Shh)

Expression Pattern of Neural Crest-Associated Genes Differs among Tissue Sources

To characterize the mRNA expression profile of neural crest cells derived from each tissue, cells from the adult P0-Cre/Floxed-

Table 1. Differentiation Potential of Spheres Derived from DRG, WP, and BM of Adult P0-Cre/Floxed-EGFP Mice

Frequency of Sphere Types (Percent ± SD)

	NGM	NM	NG	GM	N	M	G	Others
DRG	74.6 ± 1.0	21.8 ± 3.6	2.3 ± 3.2	0	1.0 ± 0.2	0	0	0
WP	7.3 ± 3.6	91.6 ± 3.1	0	0	0	1.1 ± 1.1	0	0
BM	3.3 ± 0.4	15.6 ± 0.8	0.5 ± 0.8	0.8 ± 0.7	7.3 ± 8.5	64.6 ± 11.7	0.7 ± 1.2	7.3 ± 2.6

EGFP+ spheres formed from clonal density cultures of each tissue source were differentiated and subjected to triple immunostaining. The differentiation potential of 100 spheres from each tissue source was individually examined, and each sphere's ability to differentiate into each cell type was determined: N, neurons; G, glial cells; M, myofibroblasts (mean ± SD, n = 3 per group). Spheres derived from the DRG showed a significantly higher frequency of trilineage differentiation potential (N + G + M) than the spheres from other sources (p < 0.05 by Kruskal-Willis test). Of the spheres derived from the BM, 7.3% were negative for all three lineage markers.

(Y.O. and H.O., unpublished data). These results indirectly suggest that the examined cells did not have ventral identities and do not conflict with the fact that they are developmentally derived from the dorsal neural tube, where neural crest cells originate.

EGFP+ Cells of the DRG Strongly Express NCSC Markers in Adult P0-Cre/Floxed-EGFP Mice

To quantify the expression of the NCSC markers *Sox10* and *p75* in fresh noncultured EGFP+ cells and in spheres cultured for 2 weeks, we performed real-time PCR (Figure 6B). *Sox10* and *p75* expression was higher in both the noncultured cells and cultured spheres from the DRG compared with those from the WP and BM, suggesting that there is a higher proportion of NCSCs in the DRG. However, since these genes are also expressed in specific neurons and glial cells (Kaplan and Miller, 2000; Paratore et al., 2001), we examined the expression levels of *Nestin* and *Musashi1*. Although they are used as markers for undifferentiated cells in the CNS (Lendahl et al., 1990; Sakakibara et al., 1996), they are also expressed in neural crest-derived sphere initiating cells from the heart (Tomita et al., 2005), cornea (Yoshida et al., 2006) and gut (R. Hotta, S.S., and H.O., unpublished data). Since it has been suggested that *Nestin* and *Musashi1* expression may reflect an undifferentiated state (Tomita et al., 2005), their high expression in spheres generated from the DRG also suggests that the DRG contains the highest proportion of NCSCs, and their increased expression after culture suggests that these NCSCs proliferate in culture when spheres are formed.

DISCUSSION

In the present study, by using the double-transgenic mouse strains P0 and Wnt1-Cre/Floxed-EGFP, we examined multiple tissues and organs to map the presence of neural crest-derived cells. We discovered the existence of multipotent NCSCs in the BM and DRG of adult rodents along with the previously reported facial WP. However, analysis of these cells revealed interesting differences that were specific to the tissue source. Careful consideration of these differences will be necessary if these cells are to be recruited for cell transplantation treatments.

Our histological analysis of adult P0 and Wnt1-Cre/Floxed-EGFP mice revealed EGFP+ cells in the BM (Figure 1 and Figure S1). Using flow cytometry, we collected EGFP+ BM cells that proliferated to form spheres (Figure 4). Although the frequency was low, compared with the other tissue sources,

multipotent NCSCs were present in the BM. Clonal spheres with a trilineage differentiation potential into neurons, glial cells, and myofibroblasts were observed, and dissociated cells from these spheres formed secondary spheres (Figure 5, Figures S4 and S5). The presence of NCSCs in the BM is also supported by a recent report using the same P0-Cre reporter mice to demonstrate that a portion of MSCs in the BM of the lower extremities are of neural crest lineage (Takashima et al., 2007). Furthermore, we have unpublished data showing that NCSCs contribute to produce a subpopulation of MSCs in the BM. At the embryonic stage, NCSCs differentiate into many types of neural crest lineage cells, most of which are marked with EGFP in P0 and Wnt1-Cre/Floxed-EGFP mice. We prospectively isolated EGFP+ MSCs from the BM of P0 and Wnt1-Cre mice using flow cytometry and identified that EGFP+ MSCs could generate osteocytes, chondrocytes, and adipocytes (S.M. and Y.M., unpublished data). Together with Nishikawa's report, these findings show that a certain population of MSCs in the BM originates from multipotent NCSCs.

Since a previous report indicated that Wnt1 is expressed in the BM of adult rodents (Almeida et al., 2005), we cannot rule out the possibility that the EGFP+ labeling in the BM of adult Wnt1-Cre/Floxed-EGFP mice was due to the ongoing expression of Wnt1 in the adult BM rather than reflecting a history of Wnt1 expression in the embryonic neural crest lineage. However, we found that the sphere-forming potential and differentiation tendency of EGFP+ cells from the BM of Wnt1-Cre/Floxed-EGFP mice were similar to those from P0-Cre/Floxed-EGFP mice (Figure S4), suggesting the presence of NCSCs among the EGFP+ cells in the BM of adult Wnt1-Cre/Floxed-EGFP mice. The BM stem cells reported in other studies differentiated into neurons and glial cells in vitro and in vivo and also in transplantation experiments (Fernandez et al., 2004; Jiang et al., 2002). Although transdifferentiation or dedifferentiation has been suggested to explain this phenomenon, our results demonstrating the presence of NCSCs in the BM indicate that this differentiation potential may reflect that of NCSCs of the BM. It will be interesting to clarify the relationship between the NCSCs described in the present study and the BM-derived stem cells that are reported to generate neural cells in vitro (Kohyama et al., 2001).

Hematopoiesis is initiated in the yolk sac at the embryonic stage and is successively transferred to the AGM region, fetal liver, and BM with time (Dzierzak and Speck, 2008). Using two independent Cre lines, we detected NCSCs in the AGM region, fetal liver, and BM during a time frame that coincided with the
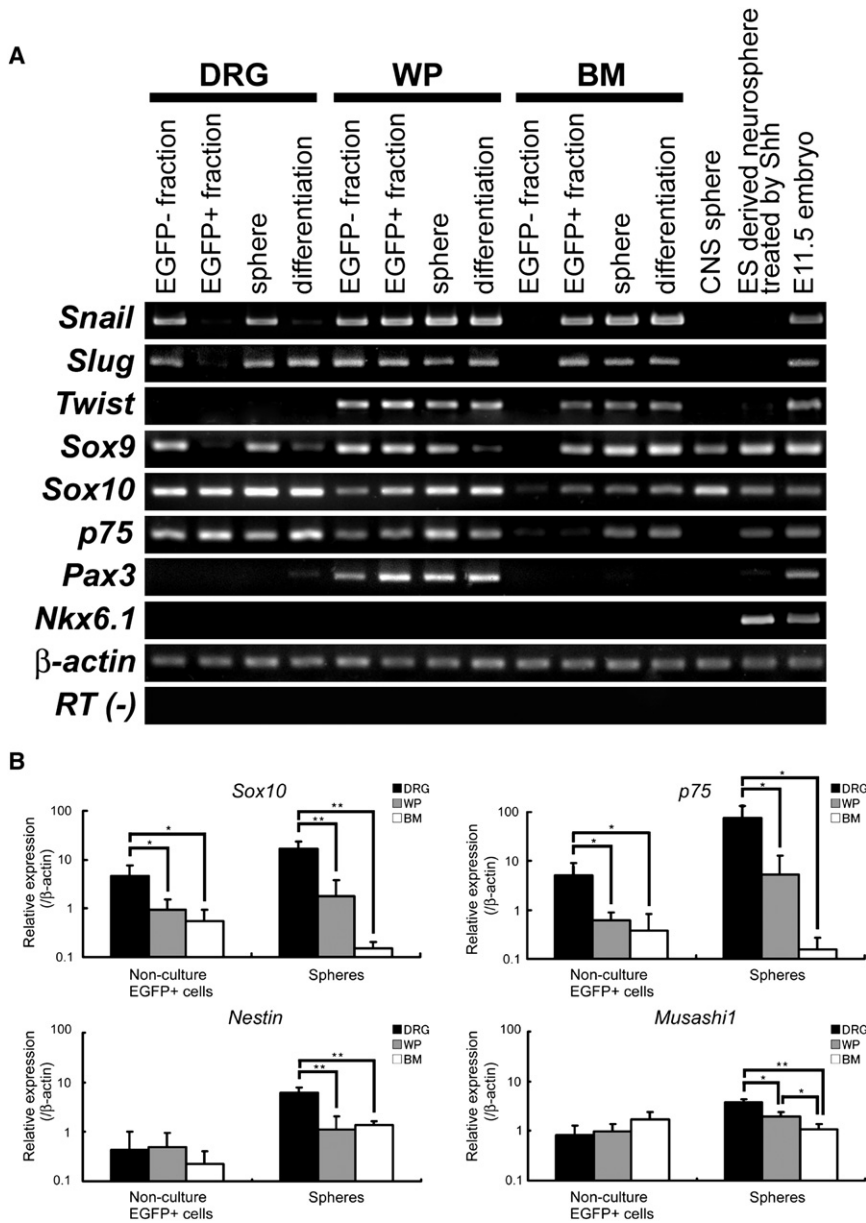
Figure 6. Expression Patterns of Embryonic Neural Crest-Specific Markers in Adult P0-Cre/Floxed-EGFP Mice

(A) Semiquantitative RT-PCR was conducted to evaluate the mRNA expression of various NCSC markers. Four types of cells were examined for each tissue source: EGFP⁻ and EGFP⁺ cells freshly fractionated by flow cytometry, EGFP⁺ spheres after 14 days in culture, and differentiated cells. Total RNA from a whole E11.5 embryo was collected as a positive control. The expression frequencies of neural crest-lineage markers from the three tissue sources were variable and quite different from the CNS-type neurospheres cultured from the striatum of an E14.5 mouse (CNS sphere). The ventral marker *Nkx6.1*, observed in ES-cell-derived neurospheres ventralized by Shh induction, was not observed in any of the EGFP⁺ neural crest-derived spheres.

(B) Quantitative PCR analysis revealed significantly higher expression of the NCSC markers *Sox10* and *p75* in the cells derived from the adult DRG. Immature stem/progenitor specific markers *Nestin* and *Musashi1* were also highly expressed in the DRG-derived spheres. *p < 0.05, **p < 0.01.

adult mice. Compared with the cells derived from the WP and BM, the neural crest-derived cells of the DRG contained a higher proportion of tripotent cells and displayed a greater ability to form secondary spheres (Figure 5 and Table 1). The expression levels of the NCSC markers *Sox10* and *p75*, and markers for undifferentiated stem/progenitor cells, *Nestin* and *Musashi1*, were also higher in the DRG-derived EGFP⁺ cells from adult P0-Cre/Floxed-EGFP mice (Figure 6B), suggesting that the DRG contained the highest proportion of NCSCs of the tissues studied. The origin of the NCSCs in the DRG is presently unknown. The DRG develops from two

period of hematopoiesis of each site, suggesting that NCSCs join the migration pathway of hematopoietic cells on the way to the BM from the embryonic period through adulthood. Our present findings concerning the migration stream of NCSCs imply an undiscovered relationship between NCSCs and hematopoiesis.

The DRG is derived from the neural crest. Although several groups have demonstrated the existence of NCSCs in the embryonic DRG (Leimeroth et al., 2002; Paratore et al., 2001), we confirmed their existence in the DRG of adult rodents. Recently, DRG-derived sphere-initiating cells were reported in adult rodents, but their origin and potential were not elucidated (Li et al., 2007). In our present study, using P0 and Wnt1-Cre reporter mice, we demonstrated that the observed cells were of neural crest lineage. Furthermore, examination of the spheres formed through a valid clonal culture method confirmed the presence of cells with stem cell-like properties in the DRG of

sources: neural crest cells that follow the ventromedial pathway and BC cells that originate from the dorsal root entry zone (Maro et al., 2004). BC cells are also neural crest-derived populations that transiently occupy the dorsal entry and ventral exit points of trunk spinal nerve roots during peripheral nervous system development (Altman and Bayer, 1984; Niederlander and Lumsden, 1996). Since embryonic BC cells include multipotent NCSCs (Hjerling-Leffler et al., 2005), it is possible that NCSCs originating from the BC migrate to and remain in the DRG until adulthood.

The presence of NCSCs in the facial skin and whisker follicle was reported previously (Fernandes et al., 2004; Sieber-Blum et al., 2004), and our results confirm their existence. An interesting finding was the formation of spheres from EGFP⁻ cells of the WP of P0 and Wnt1-Cre/Floxed-EGFP mice, although at a significantly lower percentage than the EGFP⁺ cells (Figure 4D and

Figure S4C). These EGFP⁻ spheres may develop from stem/progenitor cells with an origin other than the neural crest, such as the keratinocyte stem cells of the epithelium (Kobayashi et al., 1993). However, since the gene expression profile of EGFP⁻ cells was similar to that of EGFP⁺ cells, this seems unlikely (Figure 6A). Another possible explanation for their presence is transgene silencing through epigenetic modifications such as DNA methylation, which can weaken EGFP expression (Turker, 2002). When EGFP⁻ spheres were cultured in medium containing the demethylating agent 5-azacytidine, we observed EGFP expression in some of them (data not shown), suggesting that DNA methylation-mediated transgene silencing partially accounts for the presence of EGFP⁻ spheres.

Our results from culturing and characterizing NCSCs from the adult BM, DRG, and WP revealed significant tissue-source-dependent differences. Similarly, NCSCs from the embryonic gut and sciatic nerve exhibit heritable, cell-intrinsic differences in their responses to lineage-determination factors in vitro and in vivo (Bixby et al., 2002). Factors that come into play during the segregation, migration, and maintenance of neural crest cells have been proposed to explain these differences in NCSC characteristics. In the premigratory neural tube, a gradient of multiple signals is present along the rostrocaudal neuraxis, affecting the premigratory neural crest cells (Abzhanov et al., 2003; Lwigale et al., 2004). Once the neural crest cells separate from the neural tube, they are exposed to a multitude of factors through their path of migration, and NCSCs that survive in each respective tissue are affected by factors within that tissue (Couly et al., 2002; Trainor et al., 2002). There are also differences between embryonic and postnatal stages, as revealed in a study showing differences between fetal and adult gut NCSCs (Kruger et al., 2002). Therefore, it may be unrealistic to attempt to characterize NCSCs as a single population, since those from different sources display different traits. Instead, it will be important to understand these differences and to elucidate the molecular mechanisms for the maintenance and lineage determination of NCSCs in each tissue.

NCSCs are attracting increasing interest as potential candidates for cell transplantation therapy of nerve trauma and disease, because they are present in tissue that can be harvested from the patient. This allows for autologous transplantation, avoiding immunological complications as well as the ethical concerns associated with embryonic stem cells. We isolated and examined NCSCs from adult tissues with this in mind and discovered that NCSCs from different tissues had distinct characteristics. Further study of these NCSCs will hopefully lead to the culture and transplantation of NCSCs most appropriate for the lesion receiving treatment.

EXPERIMENTAL PROCEDURES

Animals

Transgenic mice expressing Cre recombinase under control of the P0 promoter (P0-Cre) (Yamauchi et al., 1999) and Wnt1 promoter/enhancer (Wnt1-Cre) (Danielian et al., 1998) were mated with EGFP reporter mice (CAG-CAT$^{loxP/loxP}$-EGFP) (Kawamoto et al., 2000) to obtain P0-Cre/Floxed-EGFP and Wnt1-Cre/Floxed-EGFP double-transgenic mice. Mice heterozygous for a null allele of Flt1 (Flt1$^{+/lacZ}$) (Fong et al., 1995) were crossed to P0-Cre/Floxed-EGFP double-transgenic mice to obtain P0-Cre/Floxed-EGFP/Flt1^{lacZ} triple transgenic mice. Adult wild-type mice were purchased for mating from CLEA Japan. All experimental procedures were approved by the ethics committee of Keio University and were in accordance with the Guide for the Care and Use of Laboratory Animals (U.S. National Institutes of Health).

Immunohistochemistry

For histological analysis, samples were fixed in 4% paraformaldehyde (PFA) and embedded in cryomold for sectioning at 14 μm. The following antibodies were used as primary antibodies: anti-green fluorescent protein (GFP) (rabbit IgG, 1:500, MBL, and goat IgG, 1:200, Santa Cruz Biotechnology), Sox10 (goat IgG, 1:200, R&D Systems), p75 (rabbit IgG, 1:500, Chemicon), TH (sheep IgG, 1:200, Chemicon), and P0 (chick IgG, 1:200, Aves). Immunoreactivity was visualized using secondary antibodies conjugated with Alexa 488 or Alexa 568 (Molecular Probes). Nuclear counterstaining was performed with Hoechst 33342 (10 μg/ml, Sigma B2261). The samples were observed with a confocal laser scanning microscope (LSM510, Carl Zeiss). Whole-mount preparation of tibias and immunostaining were performed as described (Kubota et al., 2008).

Preparation of DRG, WP, and BM Cells

Juvenile (14–28 days) and adult (2–12 months) P0-Cre/Floxed-EGFP mice were deeply anesthetized and sacrificed by cervical dislocation.

DRG

The vertebral body was dissected out, and the DRGs from C5 to L5 were resected into HBSS⁺ (GIBCO 14025-092) supplemented with 10% fetal bovine serum (FBS; Equitech-Bio SFB30-1478) and 1% penicillin/streptomycin (P/S; GIBCO-BRL). The peripheral nerve tissue was removed, and the DRGs were incubated with 0.25% collagenase (Sigma C5894) in HBSS⁺ for 30 min at 37°C. After being rinsed in PBS, the DRGs were incubated in 0.25% trypsin-EDTA for 30 min at 37°C and mechanically dissociated into DRG medium (neurobasal medium [GIBCO 21103-049] supplemented with 20 ng/ml B27 [GIBCO], 1% L-glucose [GIBCO], and 1% P/S). The cells were collected by centrifugation at 800 × g for 3 min at 4°C.

WP

The facial WP was carefully dissected, washed in HBSS, and incubated in 0.3% dispase II (Roche 1276921) in DMEM-F12 (GIBCO 11330-032) containing 1% P/S for 3 hr at 37°C. Hair and dermis were removed with a cell lifter (Costar). The skin tissue was minced into small pieces and digested with 0.04% collagenase (Wako 038-10531) in DMEM-F12 for 1 hr at 37°C. Cell clusters were mechanically dissociated in medium, and the suspension was poured through a 70 μm cell strainer (Falcon). The dissociated cells were collected by centrifugation at 480 × g for 3 min at 4°C.

BM

The femurs and tibias were dissected out and crushed with a pestle. The crushed bones were washed in HBSS⁺ (GIBCO 14175-095) supplemented with 2% FBS, 10 mM HEPES (GIBCO 15630-080), and 1% P/S to remove hematopoietic cells. The bone fragments were collected and incubated for 1 hr at 37°C in 0.2% collagenase (Wako 032-10534) in DMEM (GIBCO 11885-084) containing 10 mM HEPES and 1% P/S. The suspension was filtered with a cell strainer (Falcon 2350) and collected by centrifugation at 280 × g for 7 min at 4°C. The pellet was resuspended for 5–10 s in 1 ml water (Sigma W3500) to burst red blood cells, after which 1 ml of 2 × PBS (diluted from Sigma D1408) containing 4% FBS was added. The cells were resuspended in HBSS⁻, and the suspension was poured through a cell strainer.

Flow-Cytometric Analysis

Flow-cytometric analysis was performed as described previously (Matsuzaki et al., 2004). For detailed analysis of the BM in P0-Cre/Floxed-EGFP mice, BM cells were stained for 30 min on ice with PE-anti-PECAM-1 and APC-anti-CD45 (eBioscience, CA). After collecting 1 × 10⁵ events, the fluorescence intensity of PECAM-1 and EGFP in the CD45-negative cell population was plotted as a two-dimensional dot plot.

Blood cells from embryos were obtained by cutting the umbilical arteries and allowing the blood to flow freely into PBS. After collecting the PBS, EGFP⁺ cells were identified by EGFP fluorescence.

Primary and Secondary Sphere-Forming Cultures

Cells from the DRG, WP, and BM were seeded at 5 × 10³ cells/ml (Hulspas et al., 1997) in a serum-free sphere-forming medium consisting of DMEM/F-12 (1:1) (GIBCO 12100-046/21700-075) supplemented with insulin (25 μg/ml), transferrin (100 μg/ml), progesterone (20 nM), sodium selenate

(30 nM), putrescine (60 nM) (all from Sigma-Aldrich), recombinant human EGF (100 ng/ml) (Pepro Tech #100-15), human FGF-basic (100 ng/ml) (Pepro Tech #100-18b), and B27 (20 ng/ml) (modified from Reynolds and Weiss [1992]). Cells were cultured in an incubator at 37°C, 5% CO_2, and half of the medium was changed every 6–7 days. For BrdU labeling, 1 μM BrdU was added to the culture medium every 3 days. For clonal sphere expansion, the cells were cultured in the above medium with 0.8% methylcellulose (nacalai tesque 22224-55) (Yoshida et al., 2006).

For secondary sphere formation assays, primary spheres were collected, incubated in 0.25% trypsin-EDTA for 30 min at 37°C, and triturated until a single-cell suspension was obtained. The cells were spun at 860 × g for 3 min at 4°C and resuspended in the aforementioned sphere culture medium.

For statistical evaluation of the primary and secondary sphere-forming assays, one-factor ANOVA and the Tukey-Kramer test were applied.

Differentiation Analysis
Spheres were plated on poly-D-lysin/laminin (Sigma P7405/Invitrogen 23017-015)-coated 8-well chamber slides (Iwaki 5732-008) and cultured for 10 days in the following differentiation medium: DMEM/F12 (1:1) supplemented with 10% FBS, without any growth factors. For immunocytochemistry, the cells were fixed in 4% PFA and stained with the following primary antibodies: anti-GFAP (rabbit IgG, 1:500, Dako Z0334), β-III tubulin (mouse IgG2b, 1:500, Sigma T8660), αSMA (mouse IgG2a, 1:1000, Sigma A2547), and BrdU (sheep IgG, 1:500, Fitzgerald 20-BS17). Secondary antibodies were the following: anti-mouse IgG2b (Alexa 488 A-21141), anti-mouse IgG2a (Alexa 350 A-21130), anti-rabbit IgG (Alexa 568 A11036), and anti-sheep IgG (Alexa 568 A-21099 [1:1000, Molecular Probes]). The samples were observed with a universal fluorescence microscope (Axioskop 2 Plus; Carl Zeiss).

RT-PCR Assay
RT-PCR assay is described in the Supplemental Experimental Procedures. For statistical analysis, real-time RT-PCR results were evaluated using Student's t test.

SUPPLEMENTAL DATA
Supplemental Data include five figures, Supplemental Experimental Procedures, and Supplemental References and can be found with this article online at http://www.cellstemcell.com/cgi/content/full/2/4/392/DC1/.

REFERENCES
Abzhanov, A., Tzahor, E., Lassar, A.B., and Tabin, C.J. (2003). Dissimilar regulation of cell differentiation in mesencephalic (cranial) and sacral (trunk) neural crest cells in vitro. Development 130, 4567–4579.

Almeida, M., Han, L., Bellido, T., Manolagas, S.C., and Kousteni, S. (2005). Wnt proteins prevent apoptosis of both uncommitted osteoblast progenitors and differentiated osteoblasts by beta-catenin-dependent and -independent signaling cascades involving Src/ERK and phosphatidylinositol 3-kinase/AKT. J. Biol. Chem. 280, 41342–41351.

Altman, J., and Bayer, S.A. (1984). The development of the rat spinal cord. Adv. Anat. Embryol. Cell Biol. 85, 1–164.

Bhattacharyya, A., Frank, E., Ratner, N., and Brackenbury, R. (1991). P0 is an early marker of the Schwann cell lineage in chickens. Neuron 7, 831–844.

Bixby, S., Kruger, G.M., Mosher, J.T., Joseph, N.M., and Morrison, S.J. (2002). Cell-intrinsic differences between stem cells from different regions of the peripheral nervous system regulate the generation of neural diversity. Neuron 35, 643–656.

Couly, G., Creuzet, S., Bennaceur, S., Vincent, C., and Le Douarin, N.M. (2002). Interactions between Hox-negative cephalic neural crest cells and the foregut endoderm in patterning the facial skeleton in the vertebrate head. Development 129, 1061–1073.

Danielian, P.S., Muccino, D., Rowitch, D.H., Michael, S.K., and McMahon, A.P. (1998). Modification of gene activity in mouse embryos in utero by a tamoxifen-inducible form of Cre recombinase. Curr. Biol. 8, 1323–1326.

D'Ippolito, G., Diabira, S., Howard, G.A., Menei, P., Roos, B.A., and Schiller, P.C. (2004). Marrow-isolated adult multilineage inducible (MIAMI) cells, a unique population of postnatal young and old human cells with extensive expansion and differentiation potential. J. Cell Sci. 117, 2971–2981.

Dzierzak, E., and Speck, N.A. (2008). Of lineage and legacy: the development of mammalian hematopoietic stem cells. Nat. Immunol. 9, 129–136.

Etchevers, H.C., Vincent, C., Le Douarin, N.M., and Couly, G.F. (2001). The cephalic neural crest provides pericytes and smooth muscle cells to all blood vessels of the face and forebrain. Development 128, 1059–1068.

Fernandes, K.J., McKenzie, I.A., Mill, P., Smith, K.M., Akhavan, M., Barnabe-Heider, F., Biernaskie, J., Junek, A., Kobayashi, N.R., Toma, J.G., et al. (2004). A dermal niche for multipotent adult skin-derived precursor cells. Nat. Cell Biol. 6, 1082–1093.

Fernandez, C.I., Alberti, E., Mendoza, Y., Martinez, L., Collazo, J., Rosillo, J.C., and Bauza, J.Y. (2004). Motor and cognitive recovery induced by bone marrow stem cells grafted to striatum and hippocampus of impaired aged rats: functional and therapeutic considerations. Ann. N Y Acad. Sci. 1019, 48–52.

Fong, G.H., Rossant, J., Gertsenstein, M., and Breitman, M.L. (1995). Role of the Flt-1 receptor tyrosine kinase in regulating the assembly of vascular endothelium. Nature 376, 66–70.

Funk, P.E., Kincade, P.W., and Witte, P.L. (1994). Native associations of early hematopoietic stem cells and stromal cells isolated in bone marrow cell aggregates. Blood 83, 361–369.

Hjerling-Leffler, J., Marmigere, F., Heglind, M., Cederberg, A., Koltzenburg, M., Enerback, S., and Ernfors, P. (2005). The boundary cap: a source of neural crest stem cells that generate multiple sensory neuron subtypes. Development 132, 2623–2632.

Hulspas, R., Tiarks, C., Reilly, J., Hsieh, C.C., Recht, L., and Quesenberry, P.J. (1997). In vitro cell density-dependent clonal growth of EGF-responsive murine neural progenitor cells under serum-free conditions. Exp. Neurol. 148, 147–156.

Jensen, J., Serup, P., Karlsen, C., Nielsen, T.F., and Madsen, O.D. (1996). mRNA profiling of rat islet tumors reveals nkx 6.1 as a beta-cell-specific homeodomain transcription factor. J. Biol. Chem. 271, 18749–18758.

Jessberger, S., Clemenson, G.D., Jr., and Gage, F.H. (2007). Spontaneous fusion and nonclonal growth of adult neural stem cells. Stem Cells 25, 871–874.

Jiang, Y., Jahagirdar, B.N., Reinhardt, R.L., Schwartz, R.E., Keene, C.D., Ortiz-Gonzalez, X.R., Reyes, M., Lenvik, T., Lund, T., Blackstad, M., et al. (2002). Pluripotency of mesenchymal stem cells derived from adult marrow. Nature 418, 41–49.

Joseph, N.M., Mukouyama, Y.S., Mosher, J.T., Jaegle, M., Crone, S.A., Dormand, E.L., Lee, K.F., Meijer, D., Anderson, D.J., and Morrison, S.J. (2004). Neural crest stem cells undergo multilineage differentiation in developing peripheral nerves to generate endoneurial fibroblasts in addition to Schwann cells. Development 131, 5599–5612.

Kaplan, D.R., and Miller, F.D. (2000). Neurotrophin signal transduction in the nervous system. Curr. Opin. Neurobiol. 10, 381–391.

Kawamoto, S., Niwa, H., Tashiro, F., Sano, S., Kondoh, G., Takeda, J., Tabayashi, K., and Miyazaki, J. (2000). A novel reporter mouse strain that expresses enhanced green fluorescent protein upon Cre-mediated recombination. FEBS Lett. 470, 263–268.

Kobayashi, K., Rochat, A., and Barrandon, Y. (1993). Segregation of keratinocyte colony-forming cells in the bulge of the rat vibrissa. Proc. Natl. Acad. Sci. USA 90, 7391–7395.

Kohyama, J., Abe, H., Shimazaki, T., Koizumi, A., Nakashima, K., Gojo, S., Taga, T., Okano, H., Hata, J., and Umezawa, A. (2001). Brain from bone: efficient "meta-differentiation" of marrow stroma-derived mature osteoblasts to neurons with Noggin or a demethylating agent. Differentiation 68, 235–244.

Kruger, G.M., Mosher, J.T., Bixby, S., Joseph, N., Iwashita, T., and Morrison, S.J. (2002). Neural crest stem cells persist in the adult gut but undergo changes in self-renewal, neuronal subtype potential, and factor responsiveness. Neuron 35, 657–669.

Kubota, Y., Takubo, K., and Suda, T. (2008). Bone marrow long label-retaining cells reside in the sinusoidal hypoxic niche. Biochem. Biophys. Res. Commun. 366, 335–339.

Le Douarin, N.M., and Kalcheim, C. (1999). The neural crest (Cambridge: Cambridge University Press).

Leimeroth, R., Lobsiger, C., Lussi, A., Taylor, V., Suter, U., and Sommer, L. (2002). Membrane-bound neuregulin1 type III actively promotes Schwann cell differentiation of multipotent Progenitor cells. Dev. Biol. 246, 245–258.

Lemke, G., Lamar, E., and Patterson, J. (1988). Isolation and analysis of the gene encoding peripheral myelin protein zero. Neuron 1, 73–83.

Lendahl, U., Zimmerman, L.B., and McKay, R.D. (1990). CNS stem cells express a new class of intermediate filament protein. Cell 60, 585–595.

Li, H.Y., Say, E.H., and Zhou, X.F. (2007). Isolation and characterization of neural crest progenitors from adult dorsal root ganglia. Stem Cells 25, 2053–2065.

Lwigale, P.Y., Conrad, G.W., and Bronner-Fraser, M. (2004). Graded potential of neural crest to form cornea, sensory neurons and cartilage along the rostro-caudal axis. Development 131, 1979–1991.

Maro, G.S., Vermeren, M., Voiculescu, O., Melton, L., Cohen, J., Charnay, P., and Topilko, P. (2004). Neural crest boundary cap cells constitute a source of neuronal and glial cells of the PNS. Nat. Neurosci. 7, 930–938.

Matsuzaki, Y., Kinjo, K., Mulligan, R.C., and Okano, H. (2004). Unexpectedly efficient homing capacity of purified murine hematopoietic stem cells. Immunity 20, 87–93.

Medvinsky, A., and Dzierzak, E. (1996). Definitive hematopoiesis is autonomously initiated by the AGM region. Cell 86, 897–906.

Mendes, S.C., Robin, C., and Dzierzak, E. (2005). Mesenchymal progenitor cells localize within hematopoietic sites throughout ontogeny. Development 132, 1127–1136.

Morrison, S.J., White, P.M., Zock, C., and Anderson, D.J. (1999). Prospective identification, isolation by flow cytometry, and in vivo self-renewal of multipotent mammalian neural crest stem cells. Cell 96, 737–749.

Muller, A.M., Medvinsky, A., Strouboulis, J., Grosveld, F., and Dzierzak, E. (1994). Development of hematopoietic stem cell activity in the mouse embryo. Immunity 1, 291–301.

Niederlander, C., and Lumsden, A. (1996). Late emigrating neural crest cells migrate specifically to the exit points of cranial branchiomotor nerves. Development 122, 2367–2374.

Paratore, C., Goerich, D.E., Suter, U., Wegner, M., and Sommer, L. (2001). Survival and glial fate acquisition of neural crest cells are regulated by an inter-play between the transcription factor Sox10 and extrinsic combinatorial signaling. Development 128, 3949–3961.

Reynolds, B.A., and Weiss, S. (1992). Generation of neurons and astrocytes from isolated cells of the adult mammalian central nervous system. Science 255, 1707–1710.

Ross, J.J., Hong, Z., Willenbring, B., Zeng, L., Isenberg, B., Lee, E.H., Reyes, M., Keirstead, S.A., Weir, E.K., Tranquillo, R.T., et al. (2006). Cytokine-induced differentiation of multipotent adult progenitor cells into functional smooth muscle cells. J. Clin. Invest. 116, 3139–3149.

Sakakibara, S., Imai, T., Hamaguchi, K., Okabe, M., Aruga, J., Nakajima, K., Yasutomi, D., Nagata, T., Kurihara, Y., Uesugi, S., et al. (1996). Mouse-Musashi-1, a neural RNA-binding protein highly enriched in the mammalian CNS stem cell. Dev. Biol. 176, 230–242.

Shah, N.M., Groves, A.K., and Anderson, D.J. (1996). Alternative neural crest cell fates are instructively promoted by TGFbeta superfamily members. Cell 85, 331–343.

Sieber-Blum, M., Grim, M., Hu, Y.F., and Szeder, V. (2004). Pluripotent neural crest stem cells in the adult hair follicle. Dev. Dyn. 231, 258–269.

Singec, I., Knoth, R., Meyer, R.P., Maciaczyk, J., Volk, B., Nikkhah, G., Frotscher, M., and Snyder, E.Y. (2006). Defining the actual sensitivity and specificity of the neurosphere assay in stem cell biology. Nat. Methods 3, 801–806.

Stemple, D.L., and Anderson, D.J. (1992). Isolation of a stem cell for neurons and glia from the mammalian neural crest. Cell 71, 973–985.

Stolt, C.C., Lommes, P., Sock, E., Chaboissier, M.C., Schedl, A., and Wegner, M. (2003). The Sox9 transcription factor determines glial fate choice in the developing spinal cord. Genes Dev. 17, 1677–1689.

Stolt, C.C., Lommes, P., Friedrich, R.P., and Wegner, M. (2004). Transcription factors Sox8 and Sox10 perform non-equivalent roles during oligodendrocyte development despite functional redundancy. Development 131, 2349–2358.

Takashima, Y., Era, T., Nakao, K., Kondo, S., Kasuga, M., Smith, A.G., and Nishikawa, S. (2007). Neuroepithelial cells supply an initial transient wave of MSC differentiation. Cell 129, 1377–1388.

Tomita, Y., Matsumura, K., Wakamatsu, Y., Matsuzaki, Y., Shibuya, I., Kawaguchi, H., Ieda, M., Kanakubo, S., Shimazaki, T., Ogawa, S., et al. (2005). Cardiac neural crest cells contribute to the dormant multipotent stem cell in the mammalian heart. J. Cell Biol. 170, 1135–1146.

Trainor, P.A., Ariza-McNaughton, L., and Krumlauf, R. (2002). Role of the isthmus and FGFs in resolving the paradox of neural crest plasticity and prepatterning. Science 295, 1288–1291.

Turker, M.S. (2002). Gene silencing in mammalian cells and the spread of DNA methylation. Oncogene 21, 5388–5393.

Wong, C.E., Paratore, C., Dours-Zimmermann, M.T., Rochat, A., Pietri, T., Suter, U., Zimmermann, D.R., Dufour, S., Thiery, J.P., Meijer, D., et al. (2006). Neural crest-derived cells with stem cell features can be traced back to multiple lineages in the adult skin. J. Cell Biol. 175, 1005–1015.

Yamauchi, Y., Abe, K., Mantani, A., Hitoshi, Y., Suzuki, M., Osuzu, F., Kuratani, S., and Yamamura, K. (1999). A novel transgenic technique that allows specific marking of the neural crest cell lineage in mice. Dev. Biol. 212, 191–203.

Yoshida, S., Shimmura, S., Nagoshi, N., Fukuda, K., Matsuzaki, Y., Okano, H., and Tsubota, K. (2006). Isolation of multipotent neural crest-derived stem cells from the adult mouse cornea. Stem Cells 24, 2714–2722.